Journal of Cellular Physiology

N^4-aryl substituted thiosemicarbazones derived from 1-indanones as potential anti-tumor agents for breast cancer treatmen

Journal:	*Journal of Cellular Physiology*
Manuscript ID	JCP-17-0652.R1
Wiley - Manuscript type:	Original Research Article
Date Submitted by the Author:	13-Oct-2017
Complete List of Authors:	Sólimo, Aldana; Instituto de Oncologia Angel H Roffo Soraires Santacruz, Maria Cristina; Universidad de Buenos Aires Facultad de Farmacia y Bioquimica, Departamento de Farmacología, Cátedra de Química Medicinal; Consejo Nacional de Investigaciones Cientificas y Tecnicas Loaiza Perez, Andrea; Instituto de Oncologia Angel H Roffo; Consejo Nacional de Investigaciones Cientificas y Tecnicas Bal de Kier Joffé, Elisa; Instituto de Oncologia Angel H Roffo; Consejo Nacional de Investigaciones Cientificas y Tecnicas Finkielsztein, Liliana; Universidad de Buenos Aires Facultad de Farmacia y Bioquimica, Departamento de Farmacología, Cátedra de Química Medicinal Callero, Mariana; Instituto de Oncologia Angel H Roffo; Consejo Nacional de Investigaciones Cientificas y Tecnicas
Key Words:	N⁴-TSCs, HUMAN BREAST CANCER, ROS, RIBONUCLEOTIDE REDUCTASE

is globally the most common cancer as well as the leading cause of cancer deaths in women

N^4-aryl substituted thiosemicarbazones derived from 1-indanones as potential anti-tumor agents for breast cancer treatment

Sólimo A[2], Soraires SantacruzMC[1,3,4], Loaiza Perez AI[1,2], Bal de Kier Joffé E[1,2], Finkielsztein LM[3,4], Callero MA[1,2]

AFFILIATION

[1] Consejo Nacional de Investigaciones Científicas y Técnicas

[2] Universidad de Buenos Aires, Instituto de Oncología "Ángel H. Roffo", Área Investigación, Ciudad Autónoma de Buenos Aires, Argentina. Ciudad Autónoma de Buenos Aires, Argentina

[3] Universidad de Buenos Aires, Facultad de Farmacia y Bioquímica, Departamento de Farmacología, Cátedra de Química Medicinal. Ciudad Autónoma de Buenos Aires, Argentina

[4] Universidad de Buenos Aires, Facultad de Farmacia y Bioquímica, Instituto de Química y Metabolismo del Fármaco (IQUIMEFA), Consejo Nacional de Investigaciones Científicas y Técnicas. Ciudad Autónoma de Buenos Aires, Argentina

*__Address correspondence to__: Dr. Mariana A Callero. Universidad de Buenos Aires, Instituto de Oncología "Ángel H. Roffo", Área Investigación, (C1417DTB). Av. San Martin 5481, Ciudad Autónoma de Buenos Aires, Argentina. Tel: + 54-11-52875360; Fax: + 54-11-45802811. E-mail: mcallero33@gmail.com

N^4-aryl substituted thiosemicarbazones derived from 1-indanones as potential anti-tumor agents for breast cancer treatment

Introduction

Breast cancer is globally the most common cancer as well as the leading cause of cancer deaths in women (Wang et al. 2016). Nowadays, there are several treatments for breast cancer. Early stage breast cancers can be completely resected by surgery. Over time however, the disease may come back even after complete resection, which has prompted the development of an adjuvant therapy (post-surgery). Surgery followed by adjuvant treatment has been the gold standard for breast cancer treatment for a long time. More recently, neoadjuvant treatment (pre-surgery) has been recognized as an important strategy in biomarker and target evaluation (Miller et al. 2014). The choice of appropriate therapy depends mainly on the type of tumor.

There are currently three prognostic and predictive biomarkers used in routine clinical management of patients with breast cancer. They include estrogen receptor-alpha (ERα), progesterone receptor (PR), and HER2 oncogene/oncoprotein. Unfortunately, a large number of patients are resistant to current treatments, and even those that prove to be sensitive at first may eventually become resistant later. In order to overcome this obstacle, in the last years different molecules have appeared that try to overcome this resistance, optimizing the treatment strategy.

Thiosemicarbazones (TSCs) are derivatives of imines which are formed when an aldehyde/ketone reacts with a thiosemicarbazide through a condensation reaction. Lately, great emphasis is laid on the synthesis and development of these derivatives because of the wide variety of pharmacological activities they exhibit. TSCs have many biological activities based on their ability to form complexes with metals such as iron, which results in reactive oxygen species (ROS) generation. It has been described that these compounds not only target ribonucleotide reductase (RR) (Finch et al. 1999), but also other intracellular molecules such as N-myc downstream-regulated gene-1 (NDRG1) (Chen et al. 2012) and DNA topoisomerase (top2α) (Yu et al. 2009). Furthermore, since neoplastic cells require a higher amount of essential metals for proliferation than normal cells, metal chelation becomes an interesting strategy when developing anticancer drugs.

Finkielsztein et al have developed a series of N^4-arylsubstituted TSCs derived from 1-indanones (N^4-TSCs) some of which have showed antiviral activity against the bovine viral diarrhea virus (BVDV) (Finkielsztein et al. 2008). In the present study, we investigated the anti-tumor activity of a set of three N^4-TSCs: T1 and T2 are new derivatives and T3 was previously described (Soraires Santacruz et al. 2017). The biological activity of these three compounds was assessed in the human breast cancer cell lines MCF-7, MDA-MB 231 and BT 474 which differ in their biomarkers expression pattern. The results showed that only T1 and T2 had cytotoxic effect on all cells lines by apoptosis and necrosis induction mediated by ROS formation and ribonucleotide reductase inhibition. Besides, T1 and T2 inhibited two hallmark traits of cancer cells: their ability to undergo isolated clonal growth and their capacity to migrate. Finally, all N^4-TSCs tested decreased the number of cells with mammosphere-forming capacity, suggesting that this kind of compounds could be candidates as potential anti-tumor agents.

MATERIALS AND METHODS

Chemistry

Melting points (uncorrected) were determined on a Thomas Hoover apparatus. Thin layer chromatography (TLC) was used to monitor reactions. Reactions were carried out in a Microwave Synthesis Reactor Microwave 300 Anton Paar. IR spectra were recorded as KBr pellets using a Perkin Elmer Spectrum One FT-IR spectrophotometer. ^{1}H and ^{13}C NMR spectra were recorded on a Bruker 500 MHz spectrometer. High resolution mass spectra were acquired on a Bruker micrOTOF-Q II spectrometer. 5-methyl-1-indanone was prepared according to the protocols previously described (Finkielsztein et al. 2008), 4,5-dimethoxy-1-indanone and 4-methylphenyl isothiocyanate, were purchased from Sigma-Aldrich and used as received

General procedure for the synthesis of N^4-TSCs

A mixture of the conveniently substituted 1-indanone (0.38 mmol), 85% hydrazine hydrate (21 µL), the corresponding isothiocyanate (0.43 mmol), acetic acid (20 µL) and isopropanol (0.5 mL) contained in a glass tube equipped with a screw cap and magnetic agitation was placed in a microwave synthesis reactor (Microwave 300 Anton Paar) at 90°C (30 W, 2.5 bar). Once the reaction was completed, as monitored by TLC, the obtained mixture was suspended in water (5 mL), filtered and washed with ethanol (2 mL). N^4-TSCs were recrystallized from ethanol.

5-Methylindan-1-one N-(4-methylphenyl)thiosemicarbazone. (T1)

Yield: 98%, mp: 179-180°C. IR ν/cm^{-1} (KBr): 3344 (N-H), 3302 (N-H), 1591 (C=N), 1171 (C-O), 1092 (C=S). ^{1}H NMR (CDCl3) δ ppm: 2.37 (s, 3H, CH_3), 2.41 (s, 3H, CH_3), 2.82 (m, 2H, CH_2), 3.16 (m, 2H, CH_2), 7.14 (d, J=7.9 Hz, 1H, H-Ar), 7.18 (s, 1H, H-Ar), 7.21 (d, J=8.2 Hz, 2H, H-Ar), 7.54 (d, J=8.3 Hz, 2H, H-Ar), 7.65 (d, J=7.9 Hz, 1H, H-Ar), 8.47 (s, 1H, NH), 9.26 (s, 1H, NH). ^{13}C NMR (CDCl3) δ ppm: 21.4, 22.2, 27.2, 28.7, 121.8, 124.9, 126.6, 128.9, 129.7, 136.3, 142.3, 149.5, 157.3, 174.8. HRMS (ESI) m/z $(M+H)^+$ calcd for $C_{18}H_{20}N_3S$ 310.1378, found 310.1384.

4,5-Dimethoxyindan-1-one N-(4-methylphenyl)thiosemicarbazone. (T2)

Yield: 67%, mp: 182-183°C. IR ν/cm^{-1} (KBr): 3298 (N-H), 3144 (N-H), 1590 (C=N), 1184 (C-O), 1102 (C=S). ^{1}H NMR (CDCl3) δ ppm: 2.37 (s, 3H, CH_3), 2.83 (m, 2H, CH_2), 3.18 (m, 2H, CH_2), 3.90 (s, 3H, OCH_3), 3.92 (s, 3H, OCH_3), 6.93 (d, J=8.5 Hz, 1H, H-Ar), 7.21 (d, J=8.1 Hz, 2H, H-Ar), 7.48 (d, J=8.4 Hz, 1H, H-Ar), 7.53 (d, J=8.3 Hz, 2H, H-Ar), 8.44 (s, 1H, NH), 9.23 (s, 1H, NH). ^{13}C NMR (CDCl3) δ ppm: 21.2, 25.6, 27.2, 56.4, 60.5, 112.9, 117.6, 123.0, 124.7, 129.5, 129.5, 130.7, 135.6, 136.1, 142.1, 155.0, 173.3. HRMS (ESI) m/z $(M+H)^+$ calcd for $C_{19}H_{22}N_3O_2S$ 356.1433, found 356.1456.

Cell Lines

The following human breast cancer cell lines were obtained from ATCC: MCF-7, MDA-MB 231, BT 474 and MCF-10A. They were cultured in 25 cm^2 flasks in RPMI (BT 474) or DMEM-F 12 (MCF-7and MDA-MB 231) medium supplemented with 10% fetal bovine serum, in a 5% CO_2 humidified atmosphere. MCF-10 A cells were cultured in DMEM-F

12 supplemented with 5% fetal bovine serum, 20 ng/ml EGF, 0.5 μg/ml hydrocortisone and insulin 10 μg/ml.

Proliferation assay

Breast cells grown in 25 cm^2 flasks were removed by trypsinization and seeded into 96-well culture dishes at a concentration of 1,000/2,000 cells per well. Cells were allowed to grow for 48 h at 37˚C in a humidified atmosphere containing 5% CO_2. Then cells were treated with each N^4-TSCs at the following concentrations: 0.1, 1, 10, 25 and 50 μM or with DMSO (0.1%) (control) for additional 120 h. Cell viability was determined by the MTS method. The IC_{50} (concentration expressed in μM inhibiting 50% of cell growth) were determined through non-linear regression analysis using the concentration log - response curve for each cell line in software PrismGraph 5.0

Colony formation Assay

Breast cancer cell lines were treated with each N^4-TSCs (1 or 10 μM) or DMSO 0.1% (control) for 48 h, harvested with trypsin-EDTA and counted manually in the presence of Trypan blue. Following this, cells were diluted and seeded at about 1,000 viable cells per well of a six-well plate. After incubation for 10–14 days, cells were washed with PBS twice, fixed with methanol:acetic acid for 15 min, and stained with 0.5% crystal violet for 15 min at room temperature. The colony was defined to consist of at least 20 cells. Visible colonies were counted. Colony efficiency was calculated with the following formula:

$$Colony\ efficiency = \frac{number\ of colonies}{number\ of\ seeded\ cells}$$

Cell cycle progression:

Cells were treated with each N^4-TSCs (1 or 10 μM) or DMSO 0.1% (control) for 24 h. Thereafter, they were harvested, washed in PBS, and fixed in 70% ethanol. DNA was stained by incubating cells in PBS containing propidium iodide and RNAse A. Fluorescence was measured by flow cytometry and analyzed using Cyflogic software version 1.2.1. DNA analyses allowed us to determine the cell distribution in each cell cycle phase.

Induction and quantification of apoptosis:

Apoptotic/necrotic cells were determined by acridine orange/ethidium bromide staining. Tumor cells were seeded on cover slides in 6-well plates, treated with each N^4-TSCs (1 or 10 μM) or DMSO 0.1% (control) for 48 h, and washed. Then, cells were stained with a mix containing acridine orange (10 μg/ml) plus ethidium bromide (10 μg/ml) and observed under a fluorescence microscope. Cells with green fluorescence and condensed chromatin were recorded as apoptotic while orange cells with lax chromatin were recorded as necrotic cells. Experiments were repeated ≥3x.

Apoptotic cells percentage was evaluated using "*In situ cell death detection kit*" (Roche) according to the manufacturer's protocol. Briefly, tumor cells were seeded in 6-well plates, treated with each N^4-TSCs (1 or 10 μM) or DMSO 0.1% (control) for 48 h, fixed with formaldehide for 20 minutes and permeabilized for 2 min on ice. Then cells were incubated with the reaction mixture (label and enzyme solutions, 1:10) for 60 minutes at 37C. Finally, cells were washed with PBS and fluorescence, evaluated by flow cytometry, was analyzed using Cyflogic software version 1.2.1.

Measurement of intracellular reactive oxygen species

Intracellular ROS were measured using the fluorescent dye 2´,7´-dichlorodihydrofluorescein diacetate (H2DCF-DA; Sigma) after treatment with each N^4-TSCs (1 or 10 μM) or DMSO 0.1% (control) for 3 h. DCF fluorescence intensity (measured by flow cytometry or fluorometry) is proportional to the amount of intracellular ROS. Fluorescence was analyzed using Cyflogic software version 1.2.1.

Determination of γ–H2AX Foci.

Tumor cells were seeded on cover slides in 6-well plates, treated with each N^4-TSCs (1 or 10 μM) or DMSO 0.1% (control) for 48 h, and washed. Then, cells were fixed and permeabilized with cold acetone for 2 minutes three times and blocked with 5% calf serum/PBS for 1 h at 37 °C. After blocking, the cells were incubated with anti-γ-H2AX antibody (Cell Signaling Technology, 1:500 dilution), at 4 °C overnight and then incubated with the corresponding Alexa Fluor 488 fluorescent secondary antibody (Molecular Probes,dilution 1:1000) for 1 h at room temperature in the dark. Finally, cells were stained with propidium iodide and observed under a fluorescence microscope Nikon Eclipse TE2000-S.

Mammosphere formation assay

MCF-7 or BT 474 cells, treated with each N^4-TSCs (1 or 10 μM) or DMSO 0.1% (control) for 48 h, trypsinized and grown in suspension in 6-well low attachment culture plates (Greiner Bio-One, Koln, Germany) at a density of 5,000 viable cells/ml in the presence of serum-free media supplemented with B27 and EGF. Resulting mammospheres were manually counted after 5‑8 d in culture using a Nikon eclipse TE2000-S a phase contrast inverted microscope. Mammospheres were also imaged and photographed under a phase contrast microscope Nikon Eclipse TE2000-S inverted microscope. Diameters were measured with Image J software. Fifteen to twenty fields per plate were used to calculate diameter average.

Wound Healing

To analyze the effect of N^4-TSCs on migration, MDA-MB 231 cells were seeded in 6-well plates and incubated for 48 h so as to achieve an 80-90% confluent monolayer. Cells were treated for 12 h with 1 or 10 μM N^4-TSCs. After this time had elapsed, a single scratch wound was created in the monolayer with a tip. The wound was photographed under a phase contrast microscope at time 0 and approximately 17 h later (final time, T_f). Cell migration was assessed by determining the covered area at T_0 and T_f with ImageJ software and then the percentage of migration was calculated using the following equation:

$$(T_f - T_0)/T_0.$$

We considered 4 fields per plate.

Statistical Analyses

Statistical significance between 3 or more groups was calculated by one-way analysis of variance (ANOVA) followed by Tukey´s test. Statistical analysis was performed using GraphPad InStat version 5.01 for Windows, GraphPad software, San Diego, California, USA, www.graphpad.com. Designations for statistical significance are *p<0.05, **p<0.01 and ***p<0.001

RESULTS

Chemistry

The synthetic pathway for the preparation of the N^4-TSCs (Fig 1) is based on the method previously described by us. The new derivatives **T1** and **T2** were obtained in a one-pot synthesis via a multicomponent coupling reaction, under microwave irradiation (MW). For this environmentally friendly synthesis toward new compounds, in the same pot we mixed one equivalent of the corresponding 1-indanone and an excess of 15% of isothiocyanate and hydrazine hydrate in isopropanol with a catalytic amount of acetic acid. New derivatives were obtained in good yields and the structure of compounds was confirmed by ^{1}H and ^{13}C NMR, IR and HRMS data.

T1 and T2 treatment induce specific inhibition of tumor cell growth, independently on cells receptor

In order to evaluate the cytotoxic effect of T1, T2 and T3, we compared cell viability in a panel of three human breast cancer cell lines after N^4-TSCs treatment in a range between 0 and 50 μM. These cell lines differ among each other in the expression of ER, PR and HER2/neu. While MCF-7 cells are ER+/PR+/HER2- and BT 474 cells are ER+/PR+/HER2+, MDA-MB 231 cells express neither of these receptors. As figure 2A shows, T1 and T2 induce a more marked cytotoxic effect on the three cell lines, independently on their receptor expression, showing IC_{50} values lower than 11 μM. T3 showed IC_{50} values higher than 35 μM in all cell lines tested. MCF-10A cells, a non-transformed human breast cell line, were resistant to T1, T2 and T3 treatment (IC_{50} > 0.1 mM). These findings support the hypothesis that this kind of compounds are not dependent on receptor expression but are selective towards tumor cells.

One of the hallmark traits of cancer cells is their ability to undergo isolated clonal growth. The anticancer activity of N^4-TSCs was further analyzed using a colony formation assay with the differently sensitive cell lines. As figure 2B shows, T1 and T2 treatment induced a significant inhibition of colony formation at concentrations of 10 μM on MCF-7 and MDA-MB 231 cells compared with untreated control cells, while T3 showed no effect on the clonogenic efficiency even at this high concentration. On the other hand, both T1 and T2 were capable of inducing a significant inhibition of BT 474 cells clonogenic efficiency even at the lower dose assayed (1 μM).

T1 and T2 induce cell death by apoptosis and necrosis without cell cycle perturbation

In general, cytotoxic agents induce cell death by necrosis or apoptosis. With the purpose to determine the action of N^4-TSCs on cell death we stained cells with Bromide Ethidium and Acridine Orange after a 48 h treatment. As figure 3A shows, after incubation with T1 and T2 we observed early apoptosis even at a concentration of 1 μM and late apoptosis and necrosis at 10 μM of both N^4-TSCs. On the other hand, T3 showed no effects at both concentrations in all cell lines. We also quantified the percentage of apoptotic cells after N^4-TSCs treatment with the "*In situ cell death detection kit*" which has been designed for the detection and quantification of

apoptosis at single cell level based on labeling of DNA strand breaks technology (Tunel). Flow cytometric analyses revealed that both T1 and T2 (10 μM), but not T3, induced a significant increase in the number of apoptotic cells in the three cells lines (Figure 3B), confirming the results shown by the qualitative method.

In order to determine whether T1 and T2-induced apoptosis was consequence of a previous cell cycle arrest, we investigated perturbations in the cell cycle after treating breast cancer cells with these agents. For this approach, cells were exposed to each N^4-TSCs (1 or 10 μM) or 0.1% DMSO (Control) for 24 h. As shown in figure 4, accumulation of Sub-G0 events with a concomitant decrease in G0/G1 events was only observed in MCF-7 and MDA-MB 231 cell lines after T1 or T2 treatments (10 μM). In BT 474 cells this effect was observed only with T2 (10 μM).

T1 and T2 induce ROS and inhibit ribonucleotide reductase activity

Previous studies have demonstrated that other TSCs mediate their effects through the induction of ROS (Sîrbu et al. 2017) . Consequently, we decided to investigate if N^4-TSCs induced oxidative stress. To determine whether N^4-TSCs altered intracellular ROS levels, we treated cells with T1, T2 or T3 for 3 h and exposed them to 2,7-DCF before evaluating ROS levels using flow cytometry. As figure 5 depicts, in MCF-7 and BT 474 cells, T1 and T2 increased ROS level in both concentrations, while T3 did not cause any significant change Interestingly, all N^4-TSCs treatments significantly increased ROS level in MDA-MB 231 cells.

Mammalian RR is an enzyme that catalyzes the reductive conversion of ribonucleotides to deoxy-ribonucleotides for DNA replication and repair (Håkansson et al. 2006). When RR activity is inhibited, double strand breaks (DSB) appear in DNA that precipitates serine 139 phosphorylation of histone H2AX, producing γH2AX at DSB sites (Aye et al. 2015). Therefore, in order to evaluate N^4-TSCs action on RR, we investigated γH2AX foci formation after 24h-TSC treatment. Hydroxyurea (HU) treatment was included as a positive control. As figure 6 shows, γH2AX foci appeared mainly within nuclei following treatment with T1 and T2 (1 or 10 μM) and T3 (10 μM), in the three cell lines.

***N^4*-TSCs decrease mammosphere forming capacity of MCF-7 and BT 474 cells.**

Cancer Stem Cells (CSCs) can self-renew and undergo multilineage cell differentiation to drive resistance to apoptosis triggered by extracellular stressors like radiotherapy and chemotherapy contributing to therapeutic resistance and ability to metastasize (Ghebeh et al. 2013)(Ghebeh et al. 2013)(Ghebeh et al. 2013)(Ghebeh et al. 2013)(Ghebeh et al. 2013)(Ghebeh et al. 2013)(Ghebeh et al. 2013)(Ghebeh et al. 2013)(Ghebeh et al. 2013). Furthermore, mammospheres are enriched in CSCs. Therefore, we next sought to determine whether N^4-TSCs modulate CSCs self-renewal capacity by evaluating mammosphere number and diameter after 48 h of treatment. We observed that in both cell lines with mammosphere-forming capacity (MCF-7 and BT 474), all N^4-TSCs (10 μM) significantly decreased the number of mammospheres. However, while in MCF-7 cells, mammosphere diameter was only decreased by 10 μM N^4-TSCs, only 10 μM T2 was capable of reducing this parameter in BT 474 cells (fig. 7).

T1 and T2 reduce MDA-MB 231 cell migration capacity

Tumor cell migration is a key factor in carcinogenesis and tumor metastasis. Thus, next we tested whether N^4-TSCs modulate the migration ability of MDA-MB-231 cells by performing a wound-healing assay. Interestingly after T1 and T2 treatment (10 μM), the wound gap was wider in N^4-TSCs -treated cells than in the untreated ones, indicating that T1 and T2 inhibited MDA-MB-231 cells motility (Figure 8A). As figure 8B shows, cell migration percentage decreased almost 30% with T1 and T2 respect to untreated cells.

DISCUSSION

Breast cancer is one of the most common cancers among women around the world. Although progress in treatment and early detection has led to improved survival times, some patients are resistant to treatments. Therefore, the search for new treatment alternatives is a constant challenge.

Thiosemicarbazones (TSCs) have long been a focus of interest for medicinal chemistry due to their diverge range of biological activities. Recently a variety of TSCs have been developed and examined *in vitro* and *in vivo* in clinical trials. These compounds often display potent antiproliferative effects caused by diverse mechanisms of action. In the current study, two of the N^4-aryl substituted TSCs derived from 1-indanones tested (T1 and T2) showed anti-proliferative activity against three different human breast cancer cell lines. Importantly, for an agent to be useful as an anti-cancer drug, it must show preferential anti-proliferative activity against tumor cells over normal cell-types. Hence, the selectivity of N^4-TSCs was examined in MCF-10A, a non-transformed breast cell line and we observed that T1 and T2 showed no cytotoxic effect on this cell line. Considering IC_{50} values, tumor cell lines were more sensitive to T2 than T1 although the cytotoxic effect imparted by these agents was independent of their receptor expression pattern. BT 474 cells were the most sensitive to both compounds, meanwhile they demonstrated less cytotoxic activity in MCF-7 cells. The higher sensitivity of BT 474 cells was also observed in the clonogenic efficiency, since T1 and T2 decreased their isolated clonal growth even at a concentration of 1μM, while MCF-7 and MDA-MB 231 cells clonogenic efficiency was significantly diminished only with 10 μM T1 and T2. In terms of the decreased breast cancer cells growth, it was notable that the effect of T1 and T2 was merely cytotoxic, since we only observed a significant increase in TUNEL (+) cells without any cell cycle arrest after N^4-TSCs treatment, indicating increased apoptosis. Such cytotoxicity on breast cancer cells could be really important as the induction of cytostasis would of little benefit to patients, particularly when drug administration is stopped, since it leads to tumor rebound. Considering the mechanism of action of another TSCs, it was of interest to examine the effect of the agents on ROS production and ribonucleotide reductase (RR) activity. Both T1 and T2 induced ROS formation and evoked DNA damage detected as γH2AX foci as a consequence of a RR inhibiton in tumor cell lines. This inhibition was much more potent than the positive control: treatment with hydroxyurea. Our results are in agreement with those observed by Shao et al (2006), which demonstrated that the generation of ROS by Triapine, a thiosemicarbazone under clinical trial, is involved in the quenching of the tyrosyl radical of ribonucleotide reductase small subunits, enzyme inactivation, and ultimately the antiproliferation activity of the drug. Therefore, the effects of T1 and T2-induced ribonucleotide reductase inhibition (inhibit DNA synthesis and prevent DNA repair) and DNA damage may combine synergistically to cause apoptosis. RR is

critical to all living cells, controlling cell proliferation and maintaining genomic stability. Since tumor cells generally proliferate at a faster rate than their normal counterparts, RR appears to be a legitimate target for cancer chemotherapy. Because T1 and T2 resulted more potent than the clinically used RR inhibitor hydroxyurea, the pursuit of the clinical applicability of these N^4-TSCs appears to be worthwhile.

Recent studies show that cancers arise from a small fraction of cancer initiating cells that are capable of giving rise to the heterogeneity. These capacities are in parallel with normal stem cells. Thus, these cells are named as stem cell-like cancer cells (CSCs). CSCs exist in a variety of cancers like ovarian cancer, prostate cancer, and breast cancer, and are not sensitive to standard chemotherapy and radiotherapy. CSCs are not only the initiators of cancer but also might be in charge of progression, metastasis, and the recurrence of cancer after treatment. In order to investigate the effect of N^4-TSCs on CSCs we evaluated the number of cells with mammosphere-forming capacity after N^4-TSCs treatment in MCF-7 and BT 474 cells (MDA-MB 231 cells do not form mammospheres (Iglesias et al. 2013)) and we found that T1, T2 and T3 reduced the number of these cells, being BT 474 cells again more sensitive than MCF-7 cells in accordance with the data obtained by Ozer who described that HER2 overexpression parallels to increased iron levels required for cell viability (Ozer 2016), therefore the chelation of this metal by N^4-TSCs could be another mechanism associated to anti-tumor effect impart by these compounds. It must be noticed the fact that T3 has shown an inhibitory effect against CSCs despite its lack of cytotoxic activity against tumor cell bulk. This could be of particular interest considering the key role of CSCs in metastasis and anti-tumor therapy resistance. Future in vivo experiments should confirm T3 activity as complementary therapy against breast cancer.

Tumor cell migration is another key factor for the tumor dissemination. Therefore, we also investigated whether N^4-TSCs had an effect on this property in MDA-MB 231 cells and we found an inhibitory activity on tumor cell migration caused by T1 and T2, which was detectable after 17 h indicating that these N^4-TSCs induced inhibitory activity was not due to cytotoxicity. These data are consistent with Wangpu et al who showed that thiosemicarbazones like Dp44mT and DpC had inhibitory effects on cell migration, cell-extracellular attachment, and focal adhesion formation (Wangpu et al. 2016).

In summary, we have shown that T1 and T2 have tumor-specific cytotoxic effects in breast cancer cell lines independently of their receptor expression profile, mediated by ROS generation and RR inhibition. In addition, these compounds also have inhibitory effects on mammosphere forming capacity and cell migration. Together, these results suggest that T1 and T2 could be considered as potential anti-tumor agents that could provide promising new anticancer strategies in the treatment of resistant breast tumors either as alternative or complementary therapy.

COMPLIANCE WITH ETHICAL STANDARDS

Conflict of interest

We declare we have no conflict of interest.

Funding:

This study was funded by Fundación Florencio Fiorini and Universidad de Buenos Aires.

Ethical approval:

This article does not contain any studies with human participants or animals performed by any of the authors.

REFERENCES

Aye Y, Li M, Long MJC, Weiss RS (2015) Ribonucleotide reductase and cancer: biological mechanisms and targeted therapies. Oncogene 34:2011–2021. doi: 10.1038/onc.2014.155

Chen Z, Zhang D, Yue F, et al (2012) The iron chelators Dp44mT and DFO inhibit TGF-β-induced epithelial-mesenchymal transition via up-regulation of N-Myc downstream-regulated gene 1 (NDRG1). J Biol Chem 287:17016–28. doi: 10.1074/jbc.M112.350470

Finch RA, Liu MC, Cory AH, et al (1999) Triapine (3-aminopyridine-2-carboxaldehyde thiosemicarbazone; 3-AP): An inhibitor of ribonucleotide reductase with antineoplastic activity. Adv Enzyme Regul 39:3–12. doi: 10.1016/S0065-2571(98)00017-X

Finkielsztein LM, Castro EF, Fabián LE, et al (2008) New 1-indanone thiosemicarbazone derivatives active against BVDV. Eur J Med Chem 43:1767–1773. doi: 10.1016/j.ejmech.2007.10.023

Ghebeh H, Sleiman GM, Manogaran PS, et al (2013) Profiling of normal and malignant breast tissue show CD44high/CD24lowphenotype as a predominant stem/progenitor marker when used in combination with Ep-CAM/CD49f markers. BMC Cancer 13:289. doi: 10.1186/1471-2407-13-289

Håkansson P, Hofer A, Thelander L (2006) Regulation of Mammalian Ribonucleotide Reduction and dNTP Pools after DNA Damage and in Resting Cells. J Biol Chem 281:7834–7841. doi: 10.1074/jbc.M512894200

Manuel Iglesias J, Beloqui I, Garcia-Garcia F, et al (2013) Mammosphere Formation in Breast Carcinoma Cell Lines Depends upon Expression of E-cadherin. PLoS One 8:e77281. doi: 10.1371/journal.pone.0077281

Miller E, Lee HJ, Lulla A, et al (2014) Current treatment of early breast cancer: adjuvant and neoadjuvant therapy. F1000Research. doi: 10.12688/f1000research.4340.1

Ozer U (2016) The role of Iron on breast cancer stem-like cells. Cell Mol Biol (Noisy-le-grand) 62:25–30.

Shao J, Zhou B, Di Bilio AJ, et al (2006) A Ferrous-Triapine complex mediates formation of reactive oxygen species that inactivate human ribonucleotide reductase. Mol Cancer Ther 5:586–92. doi: 10.1158/1535-7163.MCT-05-0384

Sîrbu A, Palamarciuc O, Babak M V, et al (2017) Copper(ii) thiosemicarbazone complexes induce marked ROS accumulation and promote nrf2-mediated antioxidant response in highly resistant breast cancer cells. Dalton Trans 46:3833–3847. doi: 10.1039/c7dt00283a

Soraires Santacruz MC, Fabiani M, Castro EF, et al (2017) Synthesis, antiviral evaluation and molecular docking studies of N 4 -aryl substituted/unsubstituted thiosemicarbazones derived from 1-indanones as potent anti-bovine viral diarrhea virus agents. Bioorg Med Chem 25:4055–4063. doi: 10.1016/j.bmc.2017.05.056

Wang H, Naghavi M, Allen C, et al (2016) Global, regional, and national life expectancy, all-cause mortality, and cause-specific mortality for 249 causes of death, 1980–2015: a systematic analysis for the Global Burden of Disease Study 2015. Lancet 388:1459–1544. doi: 10.1016/S0140-6736(16)31012-1

Wangpu X, Lu J, Xi R, et al (2016) Targeting the Metastasis Suppressor, N-Myc Downstream Regulated Gene-1, with Novel Di-2-Pyridylketone Thiosemicarbazones: Suppression of Tumor Cell Migration and Cell-Collagen Adhesion by Inhibiting Focal Adhesion Kinase/Paxillin Signaling. Mol Pharmacol 89:521–40. doi: 10.1124/mol.115.103044

Yu Y, Kalinowski DS, Kovacevic Z, et al (2009) Thiosemicarbazones from the Old to New: Iron Chelators That Are More Than Just Ribonucleotide Reductase Inhibitors. J Med Chem 52:5271–5294. doi: 10.1021/jm900552r

Figure 1: Schematic representation of the synthetic pathway for the preparation of the N^4-TSCs

Figure 2: Effect of *N^4*-TSCs on breast cell lines growth. (A) Concentration log-response curve: results from MTS proliferation assays examining the effects of *N^4*-TSCs on the growth of breast cell lines. Cells were incubated with each *N^4*-TSCs or DMSO (control) for 5 days. The values represent the average of three independent experiments, * $p < 0.05$ with respect to control cells. (B) Colony formation assay was done on breast cancer cell lines pre-incubated with each *N^4*-TSCs (1 and 10 μM) or DMSO (control) for 48 h. The values represent the average of three independent experiments, * $p < 0.05$ with respect to control cells.

Figure 3: Evaluation of cell death induced by *N^4*-TSCs. Cells were treated with each *N^4*-TSC (1 and 10 μM) or DMSO (control) for 48 h. (A) Acridine Orange/EtBr staining of breast cancer cell lines monolayer. Images are representative of three independent experiments. (B) Apoptotic cell percentages determined by flow cytometry using *"In situ cell death detection kit".* The values represent the average of three independent experiments, * $p < 0.05$ with respect to control cells

Figure 4: Effect of N^4-TSCs on cell cycle distribution. Cells were treated with each N^4-TSC (1 and 10 μM) or DMSO (control) for 48 h. Then they were harvested, fixed in 70% ethanol, stained with propidium iodide and analyzed by flow cytometry. (A) The values represent the average of three independent experiments. (B) Cell cycle frequency histograms correspond to one representative experiment of three; 20,000 events were analyzed.

Figure 5: Effect of N^4-TSCs on intracellular ROS level. Cells were treated with each N^4-TSC (1 and 10 μM) or DMSO (control) for 3 h. ROS level was measured by flow cytometry after incubation with 2,7-DCF. Data represent the average of at least three independent experiments, * $p < 0.05$ with respect to control cells.

Figure 6: Effect of N^4-TSCs on γ-H2AX phosphorylation. Cells were treated with each N^4-TSC (1 and 10 μM) or DMSO (control) for 48 h. H2AX foci formation was evaluated by immunofluorescence. Treatment with hydroxyurea (HU) was included as positive control. Images are representative of three independent experiments.

Figure 7: Effect of N^4-TSCs on mammosphere forming capacity. Cells were treated with each N^4-TSC (1 and 10 μM) or DMSO (control) for 48 h. Mammosphere number were evaluated after a 5-8 days culture in mammosphere formation conditions. Data represent the average of at least three independent experiments, * $p < 0.05$ with respect to control cells.

Figure 8: Effect of N^4-TSCs on cellular migration. Cells were treated with each N^4-TSC (1 and 10 μM) or DMSO (control) for 12 h. A wound was made with a yellow tip; the initial and final wound areas were measured (Tf= 18 h post wound) and analyzed with the ImageJ program. (A) Representative fields from one experiment are shown. (B) The graph shows the migration percentage for each dilution done. Values that are significantly different from controls are indicated *$p< 0.05$. Experiments were performed in triplicate.

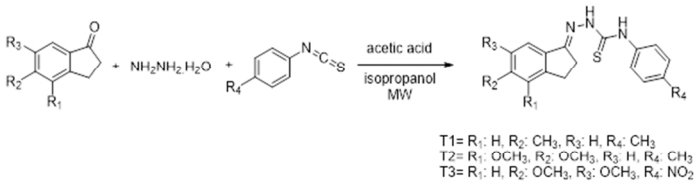

Figure 1: Schematic representation of the synthetic pathway for the preparation of the N^4-TSCs

225x56mm (96 x 96 DPI)

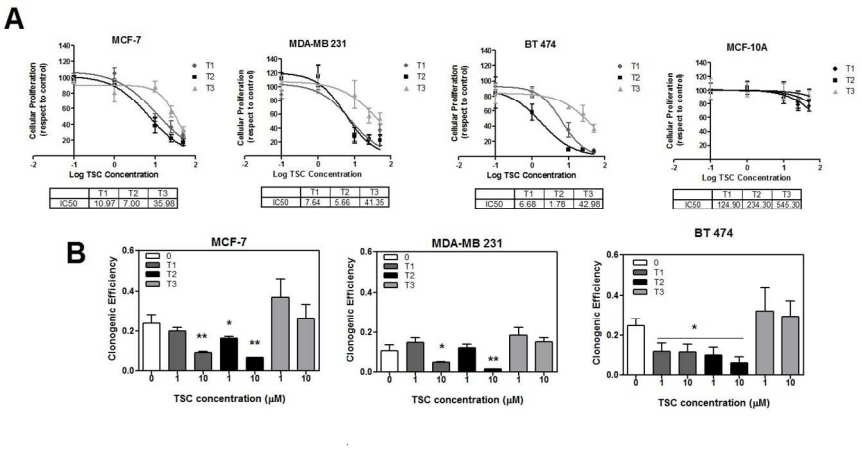

Figure 2: Effect of N^4-TSCs on breast cell lines growth. (A) Concentration log-response curve: results from MTS proliferation assays examining the effects of N^4-TSCs on the growth of breast cell lines. Cells were incubated with each N^4-TSCs or DMSO (control) for 5 days. The values represent the average of three independent experiments, * $p < 0.05$ with respect to control cells. (B) Colony formation assay was done on breast cancer cell lines pre-incubated with each N^4-TSCs (1 and 10 μM) or DMSO (control) for 48 h. The values represent the average of three independent experiments, * $p < 0.05$ with respect to control cells.

396x529mm (96 x 96 DPI)

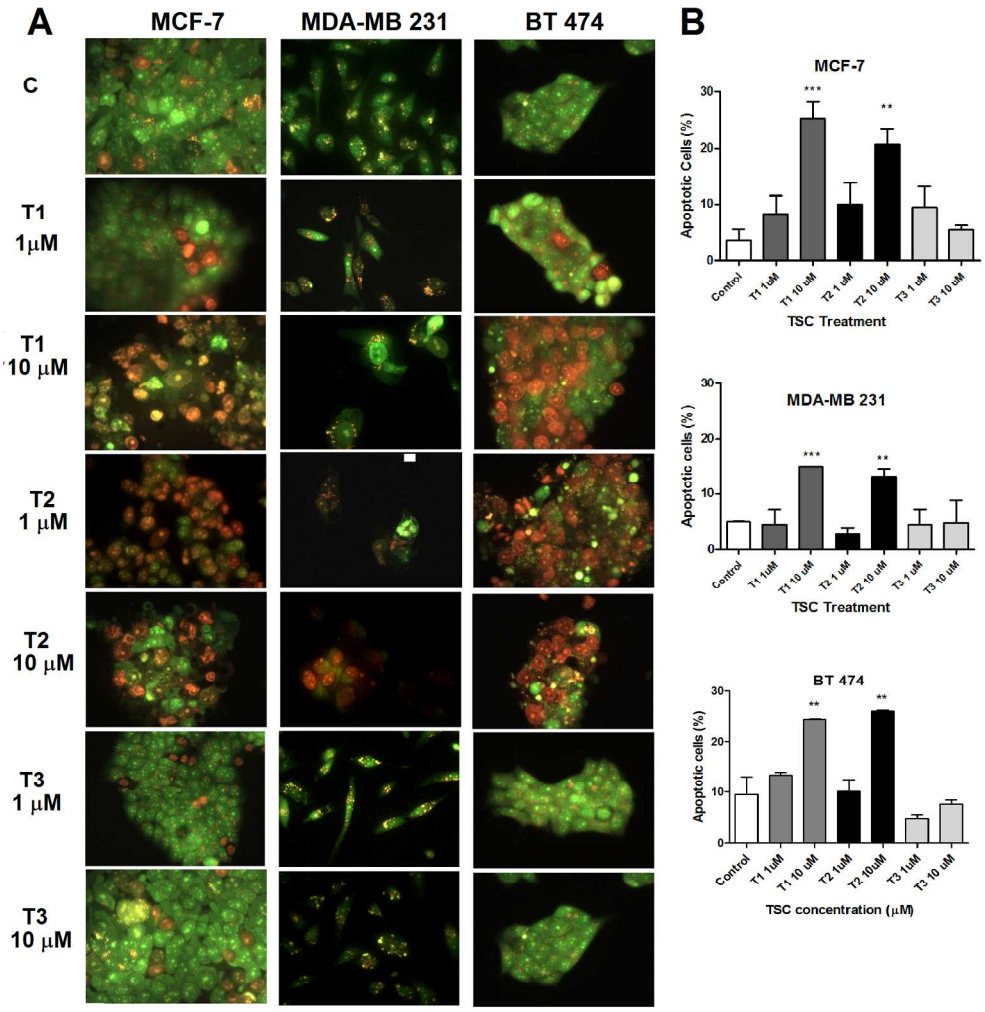

Figure 3: Evaluation of cell death induced by N^4-TSCs. Cells were treated with each N^4-TSC (1 and 10 μM) or DMSO (control) for 48 h. (A) Acridine Orange/EtBr staining of breast cancer cell lines monolayer. Images are representative of three independent experiments. (B) Apoptotic cell percentages determined by flow cytometry using "In situ cell death detection kit". The values represent the average of three independent experiments, * $p < 0.05$ with respect to control cells

576x635mm (96 x 96 DPI)

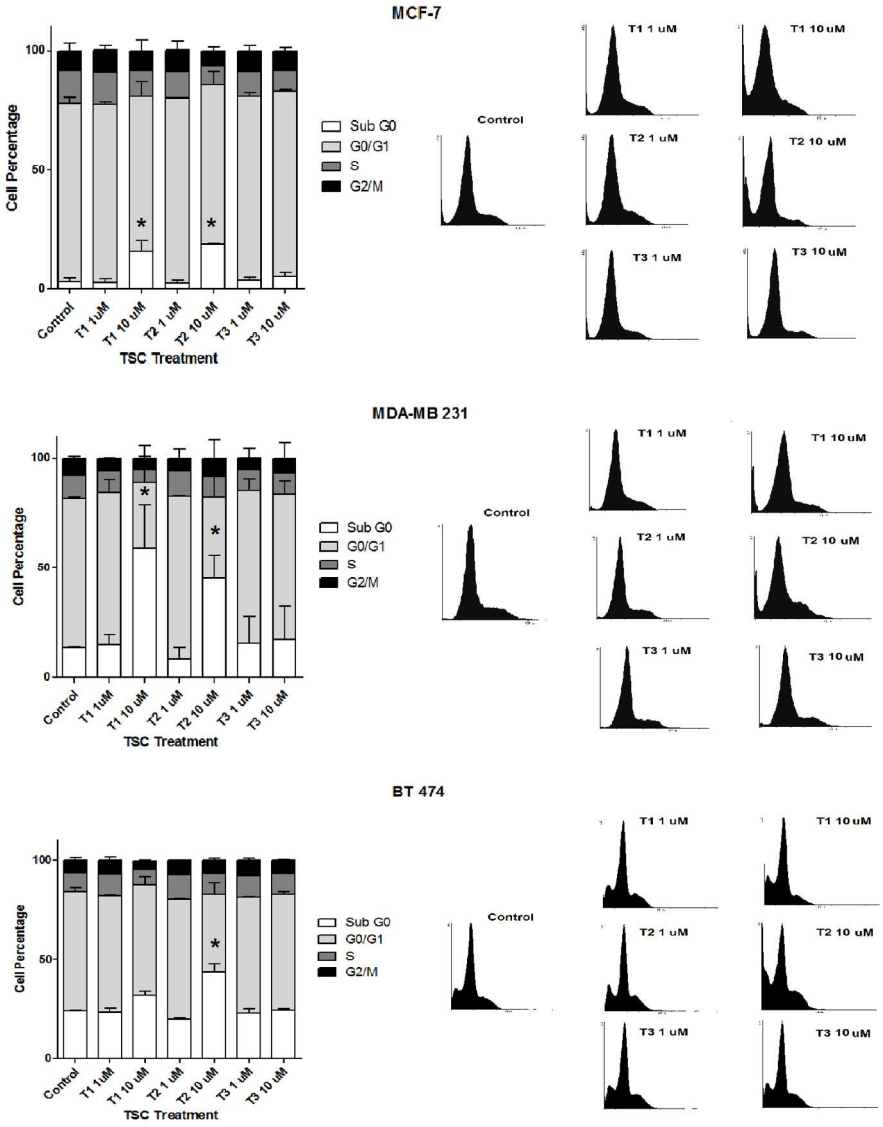

Figure 4: Effect of N^4-TSCs on cell cycle distribution. Cells were treated with each N^4-TSC (1 and 10 μM) or DMSO (control) for 48 h. Then they were harvested, fixed in 70% ethanol, stained with propidium iodide and analyzed by flow cytometry. (A) The values represent the average of three independent experiments. (B) Cell cycle frequency histograms correspond to one representative experiment of three; 20,000 events were analyzed.

462x558mm (96 x 96 DPI)

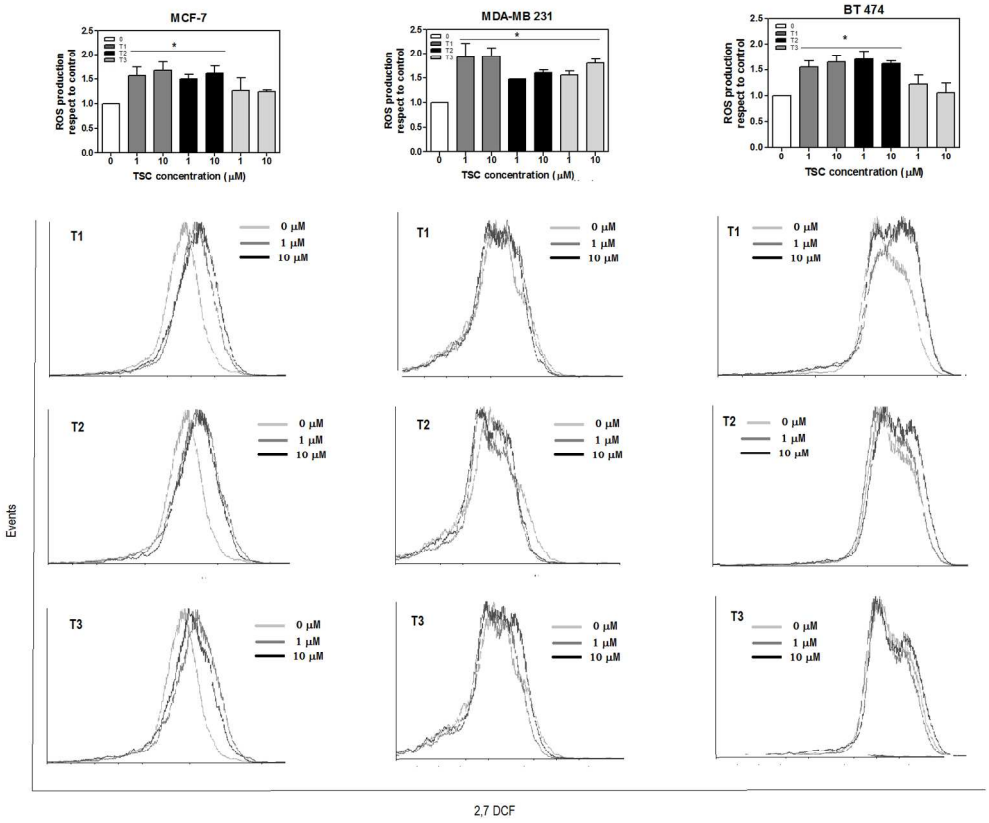

Figure 5: Effect of N^4-TSCs on intracellular ROS level. Cells were treated with each N4-TSC (1 and 10 μM) or DMSO (control) for 3 h. ROS level was measured by flow cytometry after incubation with 2,7-DCF. Data represent the average of at least three independent experiments, * $p < 0.05$ with respect to control cells.

467x415mm (96 x 96 DPI)

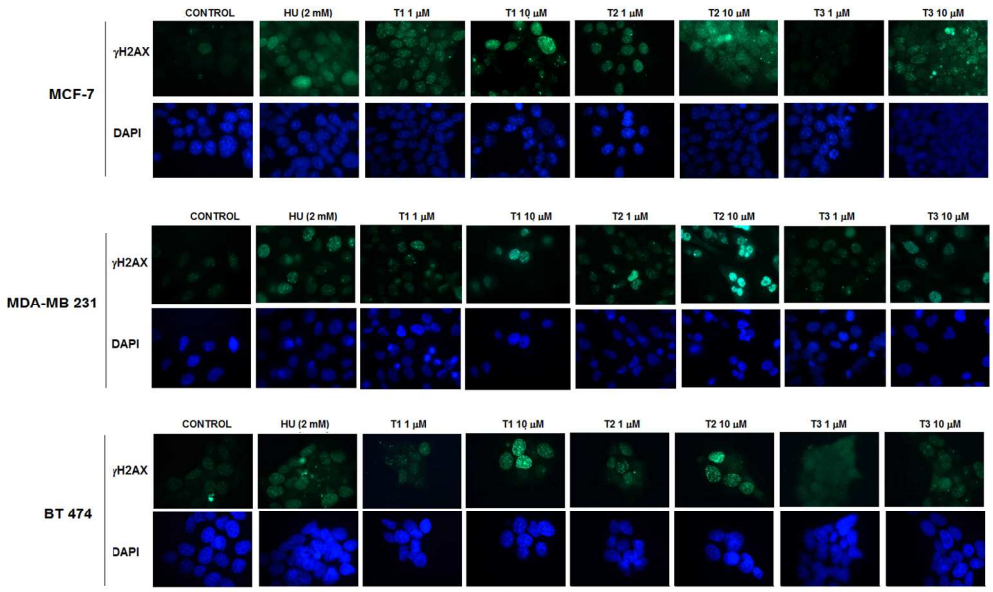

Figure 6: Effect of N^4-TSCs on γ-H2AX phosphorylation. Cells were treated with each N4-TSC (1 and 10 µM) or DMSO (control) for 48 h. H2AX foci formation was evaluated by immunofluorescence. Treatment with hydroxyurea (HU) was included as positive control. Images are representative of three independent experiments.

427x263mm (96 x 96 DPI)

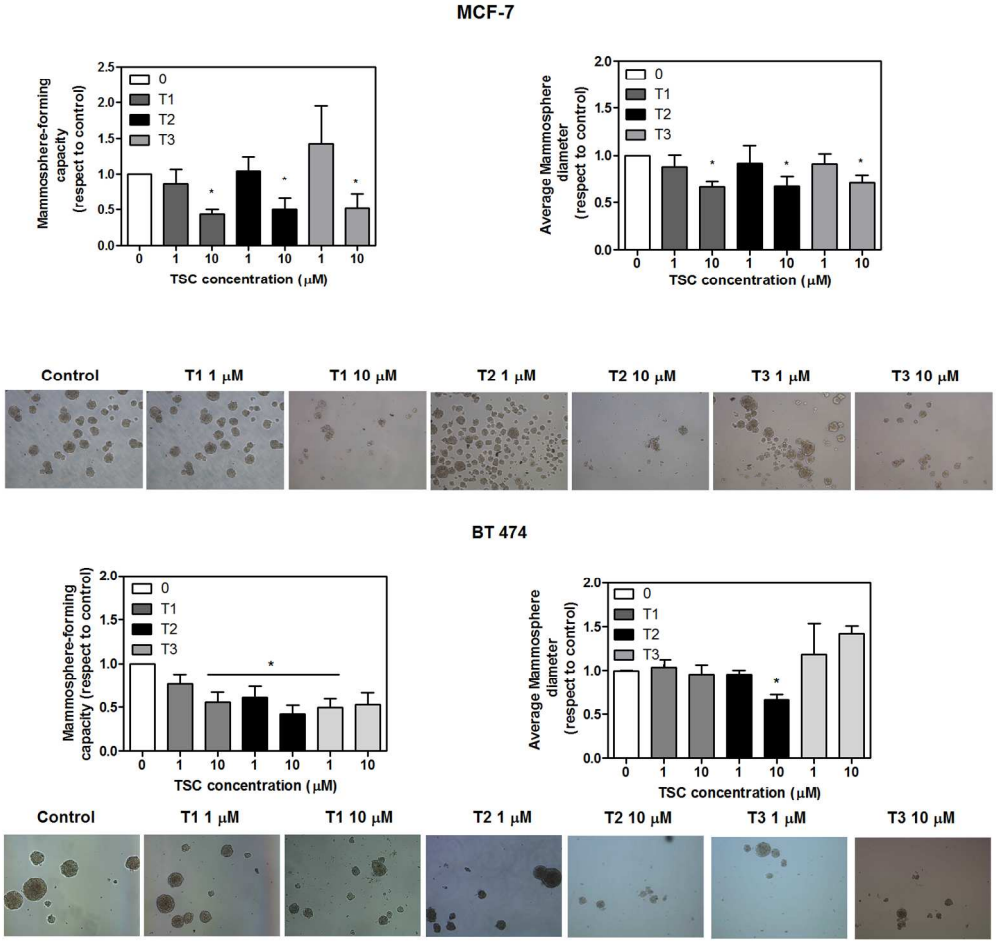

Figure 7: Effect of N^4-TSCs on mammosphere forming capacity. Cells were treated with each N^4-TSC (1 and 10 μM) or DMSO (control) for 48 h. Mammosphere number were evaluated after a 5-8 days culture in mammosphere formation conditions. Data represent the average of at least three independent experiments, * $p < 0.05$ with respect to control cells.

450x538mm (96 x 96 DPI)

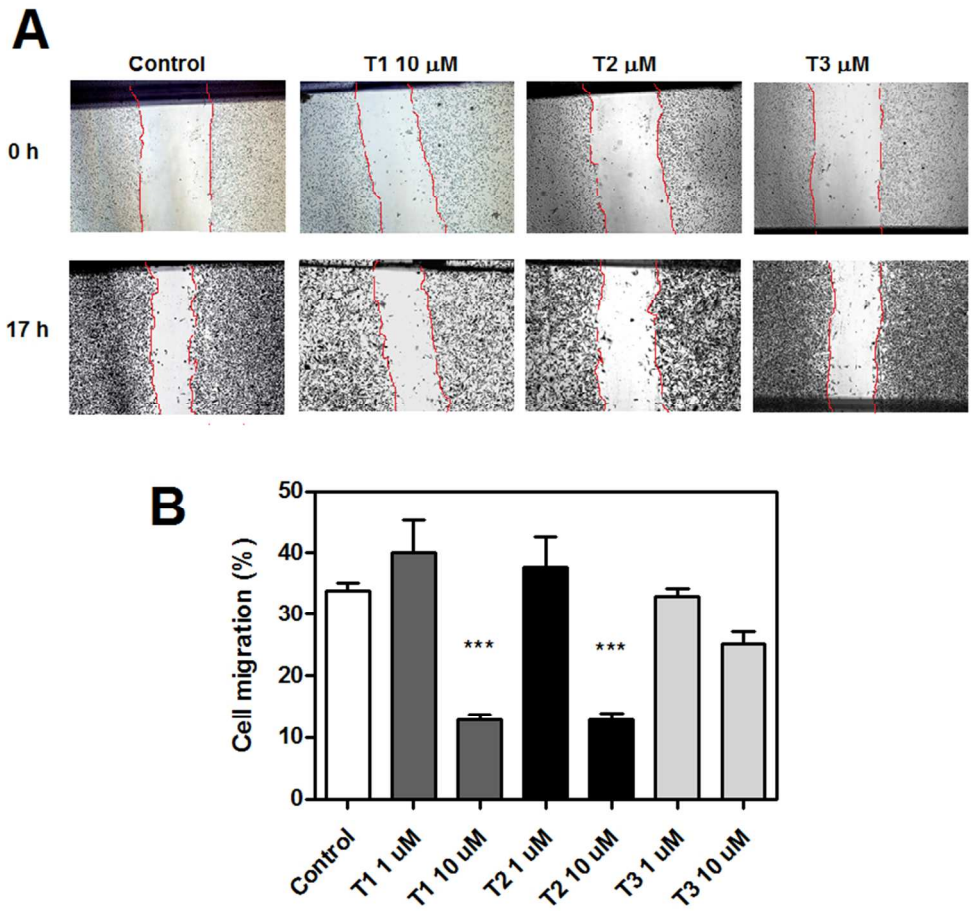

Figure 8: Effect of N^4-TSCs on cellular migration. Cells were treated with each N^4-TSC (1 and 10 µM) or DMSO (control) for 12 h. A wound was made with a yellow tip; the initial and final wound areas were measured (Tf= 18 h post wound) and analyzed with the ImageJ program. (A) Representative fields from one experiment are shown. (B) The graph shows the migration percentage for each dilution done. Values that are significantly different from controls are indicated *p< 0.05. Experiments were performed in triplicate.

237x221mm (96 x 96 DPI)